

# Critical flux pinning and enhanced upper-critical-field in magnesium diboride films

Milind N. Kunchur,<sup>\*</sup> Cheng Wu, Daniel H. Arcos, and Boris I. Ivlev<sup>†</sup>

*Department of Physics and Astronomy  
University of South Carolina, Columbia, SC 29208*

Eun-Mi Choi, Kijoon H.P. Kim, W. N. Kang, and Sung-Ik Lee

*National Creative Research Initiative Center for Superconductivity  
and Department of Physics  
Pohang University of Science and Technology  
Pohang 790-784, Republic of Korea  
(Dated: November 2, 2018)*

We have conducted pulsed transport measurements on *c*-axis oriented magnesium diboride films over the entire relevant ranges of magnetic field  $0 \lesssim H \lesssim H_{c2}$  (where  $H_{c2}$  is the upper critical field) and current density  $0 \lesssim j \lesssim j_d$  (where  $j_d$  is the depairing current density). The intrinsic disorder of the films combined with the large coherence length and three-dimensionality, compared to cuprate superconductors, results in a six-fold enhancement of  $H_{c2}$  and raises the depinning current density  $j_c$  to within an order of magnitude of  $j_d$ . The current-voltage response is highly non-linear at all fields, resulting from a combination of depinning and pair-breaking, and has no trace of an Ohmic free-flux-flow regime.

PACS numbers: 74.25.Sv, 74.25.Fy, 74.25.Bt

## I. INTRODUCTION

Magnesium diboride ( $\text{MgB}_2$ ) recently made an impact as a promising new superconductor with a surprisingly high critical temperature  $T_c$  for a simple binary compound. Besides the temperature  $T$ , the other principal parameters that define the operational space of a superconductor are magnetic field  $H$  and current density  $j$ . Superconductivity perishes above  $H_{c2}(T, j)$  and  $j_d(T, H)$ . For most practical applications it is not sufficient for the system to be merely in a superconducting state (presence of a finite order parameter amplitude) but for the system to be in a dissipationless state (constancy of order-parameter phase difference across sample length). Thus from a practical standpoint, the conventional critical current density  $j_c$  is limited by the depinning of vortices and their consequent motion. In the high- $T_c$  cuprates, the large  $T_c$  is accompanied by high values<sup>1</sup> of  $j_d$  ( $> 10^8$  A/cm<sup>2</sup>). However the layered structure and small coherence length  $\xi$  lead to very weak vortex pinning. Thus between  $j_c$  and  $j_d$ , there can be a broad dissipative regime<sup>2</sup>.

$\text{MgB}_2$  has an intermediate  $T_c$  and low values of  $j_d$  and  $H_{c2}$ .  $j_d \sim 10^7$  A/cm<sup>2</sup> at low temperatures and, in single crystals,  $H_{c2} \sim 3$  T parallel to the *c*-axis<sup>4</sup>. In the films studied here, the intrinsic disorder makes two striking improvements. First of all  $H_{c2}$  is enhanced six-fold. Secondly, pinning is enhanced to the point of raising  $j_c$  to the same order of magnitude as  $j_d$ . These observations are consistent with the reduction of  $\xi$  with disorder. Finally  $\text{MgB}_2$ 's normal-state resistivity  $\rho_n$  is lower than that of a typical cuprate superconductor (e.g.,  $\text{Y}_1\text{Ba}_2\text{Cu}_3\text{O}_7$ ) by two orders of magnitude. This increases the vortex viscosity by the same factor, so that even when the vortices are depinned, they flow at very low velocities causing insignificant dissipation until  $j_c$  becomes comparable to  $j_d$ . All these factors lead to an extremely steep non-linear current-voltage (*IV*) curve with a complete absence of an Ohmic regime characteristic of free flux flow<sup>5</sup>.

## II. EXPERIMENTAL DETAILS

An amorphous boron film was deposited on a (1 $\bar{1}$ 02)  $\text{Al}_2\text{O}_3$  substrate at room temperature by pulsed-laser ablation. The boron film was put into a Nb tube with high-purity Mg metal (99.9%) and the Nb tube was then sealed using an arc furnace in an argon atmosphere. Finally, the tube was heated to 900° C for 30 min. in an evacuated quartz ampoule sealed under high vacuum. X-ray diffraction indicates a highly *c*-axis-oriented crystal structure normal to the substrate surface with no impurity phases. The films were photolithographically patterned down to narrow bridges. In this paper we show data on three bridges, labelled S, M, and L (for small, medium, and large) with lateral dimensions 2.8 x 33, 3.0 x 61, and 9.7 x 172  $\mu\text{m}^2$  respectively. The lateral dimensions are uncertain by  $\pm 0.7 \mu\text{m}$  and the thickness by  $\pm 50$  nm. Fig. 1(a) shows the sample geometry. The horizontal sections of the current leads add a  $\sim 15$  % series resistance to the resistance of the actual bridge, which enters in measurements made at very small  $j$ . At high  $j$  in the mixed state, the extra contribution is frozen out because the current is spread out in these wider areas, diluting its density, so that one observes mainly the resistance of the bridge (A more intricate contact geometry was prohibited because of the extreme difficulty we faced in etching  $\text{MgB}_2$ ).

The non-linear electrical transport measurements were made using a pulsed signal source with pulse durations ranging from 0.1 to 4  $\mu\text{s}$  and a duty cycle of about 1 ppm. At the other extreme, a conventional continuous DC method at a very low current ( $I = 1.4 \mu\text{A}$ ) was employed for the resistive traces used to determine  $H_{c2}$ . Fig. 1(b) shows pulse waveforms under the especially severe conditions of  $j = 9.7$  MA/cm<sup>2</sup>,  $E = 83$  V/cm, and  $p = jE = 803$  MW/cm<sup>3</sup>. The resistance rises to 90% of its final value in about 50 ns from the 10% onset of  $I$ . From a knowledge of the thermal conductivities and specific heat capacities of the film and substrate materials, and their mutual thermal boundary resistance, one can calculate the total thermal resistance  $R_{th}$  for any pulse duration<sup>2,8</sup>. Also if  $R(T)$  has enough variation, the film's own resistance can be used as a thermometer to measure  $R_{th}$ . For films of  $\text{Y}_1\text{Ba}_2\text{Cu}_3\text{O}_7$  (YBCO) on  $\text{LaAlO}_3$ , which were used for most of our previous work, we found  $R_{th} \sim 1\text{--}10$  nK.cm<sup>3</sup>/W at microsecond timescales<sup>2,9,10</sup>. In the case of our  $\text{MgB}_2$  films, we expect  $R_{th}$  to be smaller because of sapphire's very high conductiv-

The samples are 400 nm thick films of  $\text{MgB}_2$  fabricated using

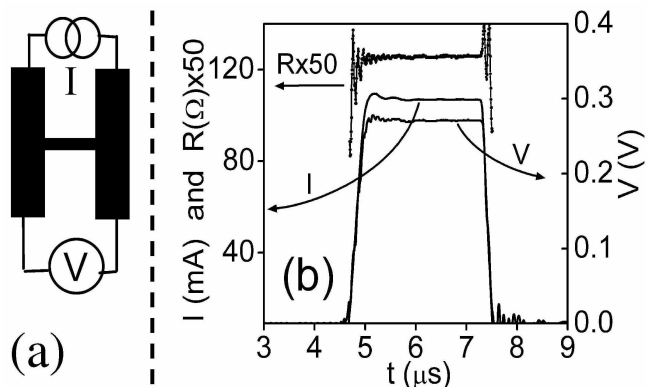


FIG. 1: (a) Sample geometry used for resistance measurement. At low values of  $j$  the wide lead areas add a constant resistance of about 15% of the total value. At high  $j$  this contribution is frozen out. (b) Pulse waveforms under worst-case conditions ( $j = 9.7 \text{ MA/cm}^2$ ,  $E = 83 \text{ V/cm}$ , and  $p = jE = 803 \text{ MW/cm}^3$  on the plateaus). The resistance rises to (90% of) its final value in about 50 ns from the (10%) onset of  $I$ .

first principles are not all known for this film-substrate combination and  $\text{MgB}_2$  has a very flat  $R(T)$  below 50 K, so one can't measure  $R_{th}$  as was done for YBCO. We can, however, obtain an upper bound on  $R_{th}$  in the following way: Fig. 2(a) shows  $IV$  curves for sample L in zero field (This is the largest sample with the lowest surface-to-volume ratio, so that it represents the worst case thermal scenario.). The curves were measured with the sample in different thermal environments. Above some threshold current  $I_d \sim 650 \text{ mA}$ , the system abruptly switches into the normal state. The value of  $I_d$  is not sensitive to the thermal environment contacting the exposed surface of the film, confirming that the highly conductive sapphire, together with the greatly reduced heat input during the short pulse, prevents the film's temperature from rising significantly (It has been shown by Stoll et al.<sup>11</sup> that if there is sample heating, the thermal environment makes a significant difference because it will provide an additional path for the heat to flow through.). Fig. 2(b) shows the top portion of one of the  $IV$  curves. The resistance jumps directly to the full normal-state value (The arrow indicates the first data point with non-zero resistance; the dashed line corresponds to  $V = R_n I$ ). It is argued elsewhere<sup>3</sup> that this jump to the normal state occurs due to pairbreaking by the current<sup>15</sup>. At the point the system is just driven normal, the power density reaches  $p = jE = 1.01 \text{ GW/cm}^3$  (arrow in Fig. 2(b)). This sets a gross upperbound of  $R_{th} \sim 7 \text{ nK.cm}^3/\text{W}$ . Note that the main bottle neck of heat conduction is the film-substrate boundary resistance which is not strongly temperature dependent<sup>8</sup>. In the present work, typical  $p$  values are two orders of magnitude lower than the critical  $1 \text{ GW/cm}^3$  and so we expect the temperature rise to be a small fraction ( $\sim 1\%$ ) of  $T_c$ .

The magnetic field is applied normal to the film (parallel to the  $c$  axis) and the self field of the current ( $< 50 \text{ G}$ ) is much lower than the applied fields used in this work. Further details of the measurement techniques have been published in a previous review article<sup>2</sup> and other recent papers<sup>9,10</sup>.

### III. RESULTS AND ANALYSIS

Fig. 3 shows the resistive transitions at a low continuous current of  $I = 1.4 \mu\text{A}$  in different fixed magnetic fields. Panel (a) shows the full curves for sample M, whereas for sample S we

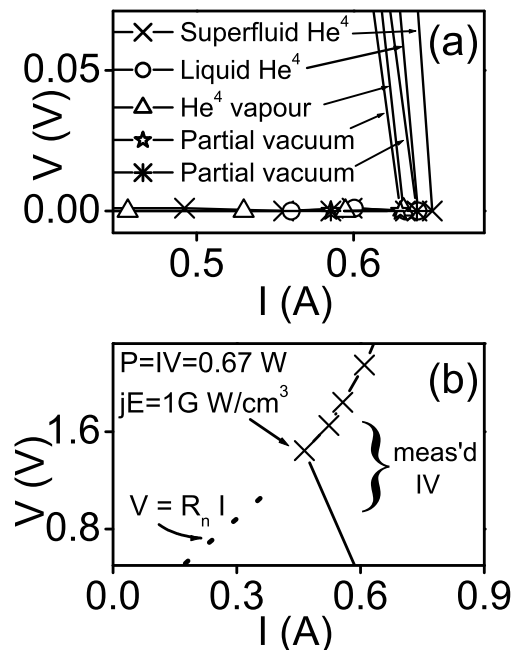


FIG. 2: Zero-field  $IV$  curves for sample L show an abrupt switch to a state of full normal-state resistance,  $R_n$ , by currents of pair-breaking magnitudes. (a) The switch to a dissipative state is not significantly influenced by the thermal environment. (b) Top portion of the curve in superfluid  $\text{He}^4$ . The resistive portion of the measured curve extrapolates to the  $V = R_n I$  dashed line.

full and central views look very similar for all three samples. In the central region, the shifts are approximately parallel, reducing the ambiguity of  $H_{c2}(T)$  defined by the transition-midpoint criterion. Fig. 4 shows those  $H_{c2}(T)$  values.  $H_{c2}(T)$  has an unusual linear dependence that departs noticeably from the dashed line of the WHH (Werthamer-Helfand-Hohenberg) function<sup>12</sup>. This observation is consistent with that of a dirty two-gap superconductor<sup>13</sup>. Panel (b) shows  $H_{c2}(T)$  for sample S defined by other criteria (see Fig. 3(b) above). Note that the linear dependence is preserved and the slopes (and hence the inferred zero- $T$  values of  $H_{c2}$ ) do not change significantly with the choice of criteria. We infer a value of  $17 \pm 3 \text{ T}$  for  $H_{c2}(0)$ , which is six times higher than the value of  $3 \text{ T}$  found in single crystals<sup>4</sup>. This can be understood in view of the much higher resistivity and hence shorter coherence length  $\xi$ : For a dirty superconductor  $\xi \approx \sqrt{\xi_0 l}$ , where  $\xi_0$  is the clean-limit value of  $\xi$  and  $l$  is the impurity scattering mean-free-path. Since  $\rho \propto l$  and  $H_{c2} \propto 1/\xi^2$ , we expect  $H_{c2} \propto \rho$ . The normal resistivity of our film samples ( $14 \mu\Omega\text{-cm}$ ) is about seven times higher than the value ( $2 \mu\Omega\text{-cm}$ ) of the single crystals of Ref.<sup>4</sup>. Note that this  $H_{c2}$  enhancement occurs naturally in the as-prepared films without any special effort to introduce pinning sites. The microscopic cause of the enhanced scattering leading to the higher  $H_{c2}$  in these samples is presently not clear.

We now turn to the in-field  $IV$  curves to investigate the nature of flux motion. In a system with weak flux pinning, the resistance goes through alternate regimes of Ohmic ( $V \propto I$ ) and non-Ohmic behavior. At very low driving forces (low  $j$ ) there can be observable resistance due to thermally activated flux flow (TAFF) or flux creep. Then one encounters a non-linear response as current-driven depinning sets in; in effect the number of mobile vortices is rising. This is incipient flux flow. At sufficiently larger  $j$ , the vortex motion is effectively free from the influence of pinning and the response becomes Ohmic again. We previously introduced the term *free flux*

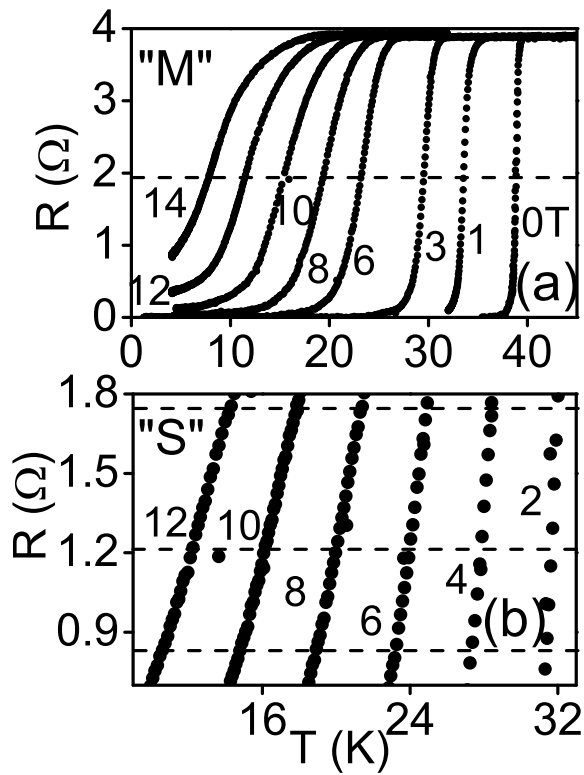


FIG. 3: Resistive transitions of two  $\text{MgB}_2$  bridges at indicated flux densities.  $I = 1.4 \mu\text{A}$ . (a) Sample M; midpoint  $T_c$ 's lie on the dashed line through  $R = R_n/2 = 1.95 \Omega$ . (b) Similar set for sample S. Dashed lines run through  $R = R_n/2 = 1.22 \Omega$ , and also through the lower and higher resistive criteria  $R = 0.84 \Omega$  and  $R = 1.76 \Omega$ .

resistivity should correspond to the canonical  $\rho_f \sim \rho_n B/H_{c2}$  Bardeen-Stephen expression<sup>16</sup>. As one goes beyond FFF, non-linearity can set in because of heating of the electron gas<sup>9</sup> or changes in the electron distribution function<sup>14</sup>. Finally at yet higher currents, pair-breaking destroys superconductivity and drives the system normal. Here the resistance again ceases to change with current, being characteristic of the normal state, and so the response becomes Ohmic one more time. These stages of dissipation have been described in our previous review article<sup>2</sup>. In  $\text{Y}_1\text{Ba}_2\text{Cu}_3\text{O}_7$ , the depinning critical current is sufficiently weak compared to the pair-breaking value that all of the regimes can be observed.

In  $\text{MgB}_2$  the situation is very different. Fig. 5(a) shows the  $R(I)$  curves of the present  $\text{MgB}_2$  samples. After the onset of dissipation, the resistance quickly rises to the full normal-state value. It should be noted that the plateaus do not correspond to FFF but to the normal state. Accordingly the resistance value changes very little with the applied  $B$ , especially for the curves at lower fields<sup>17</sup>. The overall shapes of the curves are almost independent of field. When the curves of the previous panels are shifted vertically and horizontally by constant amounts they can be made to overlap as shown in Fig. 5(b).

Fig. 6 shows the raw and shifted curves for the other two samples.

These steep IV characteristics in  $\text{MgB}_2$  are similar to those for niobium alloys but are markedly different from those in the cuprates. The latter can be understood in terms of  $\text{MgB}_2$ 's lower temperature scale and much greater pinning (due to its higher isotropy and ten times larger vortex cross section). Hence thermal activation and current driven depinning are de-

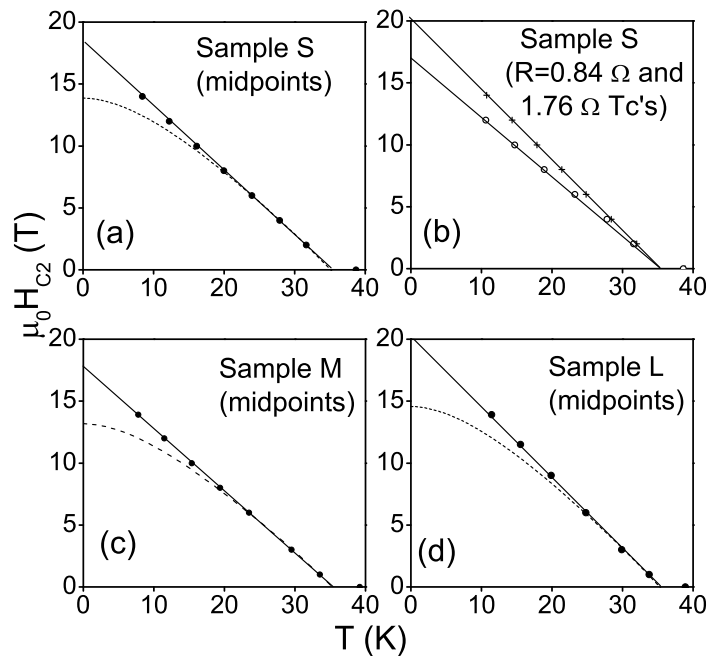


FIG. 4:  $H_{c2}$  versus  $B$  for three samples. The solid straight lines are linear fits to the data. The dashed lines correspond to the WHH function. Panel (b) shows  $H_{c2}$  for sample S defined at two other criteria. The linear behavior of  $H_{c2}(T)$  continues to hold for the  $R = 0.84 \Omega$  and  $R = 1.76 \Omega$  criteria.

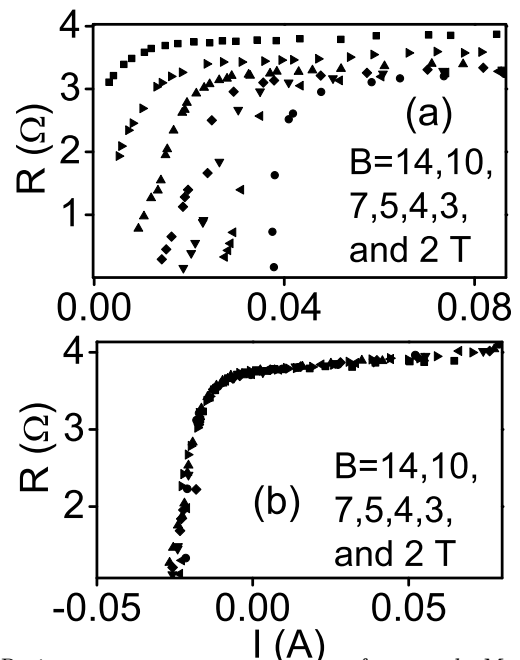


FIG. 5: Resistance versus current curves for sample M. Flux densities are indicated from left to right. The sample was immersed in superfluid helium and  $T = 1.5 \text{ K}$  for all data. (a) Raw data. (b) Same data linearly shifted so as to collapse onto a single common curve.

response to become steeply non-linear, rising from very little dissipation to the full normal state within a rather narrow range of currents. The collapse in Figs. 6 and 5 seems to suggest that the rise in resistance stems mainly from the intrinsic mechanisms of current- and field-induced pair-breaking, rather than from current driven depinning, even when  $B$  approaches  $H_{c2}$ . This makes  $\text{MgB}_2$ 's mixed-state response unique among

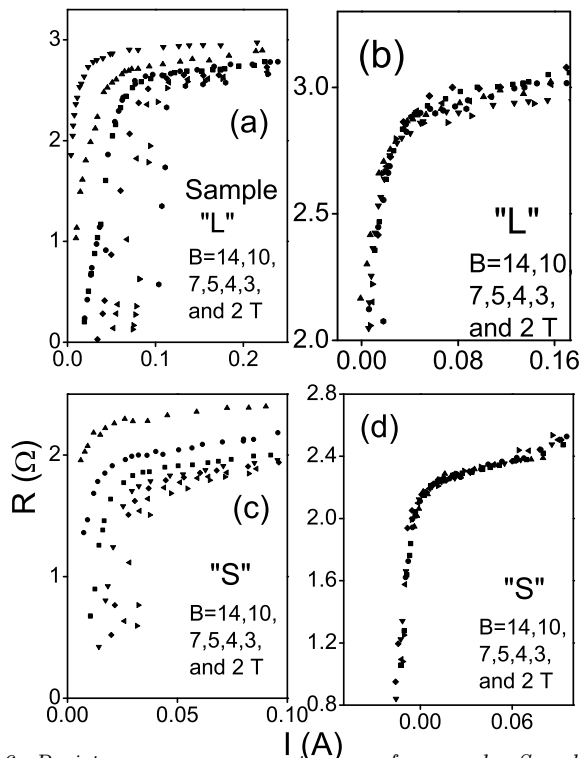


FIG. 6: Resistance versus current curves for samples *S* and *L*. Flux densities are indicated from left to right. The sample was immersed in superfluid helium and  $T = 1.5\text{K}$  for all data. Panels in the left column show raw data and panels in the right column show linearly shifted data.

applications, this implies that the practically useable current densities are much higher than might be inferred from the  $j_d$  of the material, since substantial flux dissipation is deferred until  $j_c$  becomes comparable to  $j_d$ .

## IV. CONCLUSIONS

We have investigated the low-temperature ( $T \ll T_c$ ) in-field transport behavior of  $\text{MgB}_2$  and present the first measurement of the full dissipation curves (i.e.,  $0 \leq j \lesssim j_d$  and  $0 \leq R_{T=0} \lesssim R_n$ ) for this system.  $\text{MgB}_2$  films made by the two-step laser-ablation process have an intrinsic pinning of a critical magnitude, such that the principle dissipation and resulting IV curves arise mainly from intrinsic mechanisms such as pair-breaking. The onset of dissipation is within an order of magnitude of the pair-breaking current, even at flux densities of a few teslas—the resistance rising quickly to the full normal-state value as the current is increased beyond  $j_c$ . The same disorder that enhances pinning, also enhances  $H_{c2}$  and qualitatively changes its temperature dependence because of the two-band nature of the superconductivity in this material. As explained by the theory of Gurevich,  $H_{c2}(0)$  extrapolates to a higher value than would be expected for WHH behavior, and the slope,  $dH_{c2}/dt$ , is relatively constant. Our measurements of  $H_{c2}$  are consistent with this predicted unusual dependence. Both the enhancement in  $H_{c2}$  and the critically pinned flux make such  $\text{MgB}_2$  films more promising for applications, besides providing a cleaner and more intrinsic view of a superconductor's current-voltage response in the mixed state.

## V. ACKNOWLEDGEMENTS

The authors acknowledge useful discussions with J. M. Knight and A. Gurevich. This work was supported by the U. S. Department of Energy through grant number DE-FG02-99ER45763 and by the Ministry of Science and Technology of Korea through the Creative Research Initiative Program.

\* URL: <http://www.physics.sc.edu/kunchur>; Electronic address: kunchur@sc.edu

† Also at Instituto de Física, Universidad Autonoma de San Luis Potosí, S.L.P. 78000 Mexico

<sup>1</sup> M. N. Kunchur, D. K. Christen, C. E. Klabunde, and J. M. Phillips, Phys. Rev. Lett. **72**, 752 (1994).

<sup>2</sup> M. N. Kunchur, Mod. Phys. Lett. B. **9**, 399 (1995).

<sup>3</sup> M. N. Kunchur, Sung-Ik Lee, and W. N. Kang, Phys. Rev. B. **68**, 064516 (2003).

<sup>4</sup> A. V. Sologubenko et al., Phys. Rev. B **65**, 180505(R) (2002); and O. F. de Lima et al., Phys. Rev. Lett. **87**, 47002 (2001).

<sup>5</sup> M. N. Kunchur, D. K. Christen, and J. M. Phillips, Phys. Rev. Lett. **70**, 998 (1993).

<sup>6</sup> W. N. Kang et al., Science **292**, 1521 (2001).

<sup>7</sup> W. N. Kang et al., Physica C **385**, 24 (2003).

<sup>8</sup> S. K. Gupta et al., Physica C **206**, 335 (1993) and references therein; and M. Nahum et al., Appl. Phys. Lett. **59**, 2034 (1991) and references therein.

<sup>9</sup> M. N. Kunchur, Phys. Rev. Lett. **89**, 137005 (2002).

<sup>10</sup> M. N. Kunchur, B. I. Ivlev, D. K. Christen, J. M. Phillips, Phys. Rev. Lett. **84**, 5204 (2000).

<sup>11</sup> O. M. Stoll, S. Kaiser, R. P. Huebener, and M. Naito, Phys. Rev. Lett. **81**, 2994 (2001).

<sup>12</sup> N. R. Werthamer, E. Helfand, and P. C. Hohenberg, Phys. Rev. **147**, 295 (1966).

<sup>13</sup> A. Gurevich, Phys. Rev. B **67**, 184515 (2003).

<sup>14</sup> A. I. Larkin and Yu. N. Ovchinnikov, Zh. Eksp. Teor. Fiz. **68**, 1915 (1975) [Sov. Phys. JETP **41**, 960 (1976)].

<sup>15</sup> The value of the current density at which this jump occurs,  $\sim 2 \times 10^7 \text{ A/cm}^2$ , is roughly comparable to the theoretical estimate of  $j_d(0) = cH_c(0)/[3\sqrt{6}\pi\lambda(0)] \sim 6 \times 10^7 \text{ A/cm}^2$ .

<sup>16</sup> Sometimes large departures can occur for exceptional situations such as superclean systems and narrow vortex cores where the internal energy-level spacing exceeds their widths.

<sup>17</sup> The slight shift in plateau resistance at the highest fields can be understood in terms of spreading of resistance outside the bridge area and into the current-lead areas as explained in the experimental section. Fields approaching  $H_{c2}$  start driving the whole film normal at relatively low currents so that the resistance of the wider current-lead areas is not frozen out. This causes the normal-state plateau to rise slightly at the highest fields.